Structural, magnetic, and transport properties of the electron-doped perovskites cobalt oxides $La_{1-x}Te_xCoO_3$ ($0 \leqslant x \leqslant 0.25$)

G. H. Zheng,[a] X. B. Zhu, W. H. Song, and Y. P. Sun
Key Laboratory of Materials Physics, Institute of Solid State Physics, Chinese Academy of Sciences, Hefei 230031, People' s Republic of China

(Received 27 July 2007; accepted 29 October 2007; published online 10 January 2008)

The structural, magnetic, and transport properties of the electron-doped perovskites cobalt oxides $La_{1-x}Te_xCoO_3$ ($0 \leqslant x \leqslant 0.25$) have been investigated. For the structural properties, the room temperature structural transition from rhombohedra ($R\bar{3}C$) to orthorhombic ($Pbnm$) symmetry is found in these samples with $x \geqslant 0.10$ by the Rietveld refinement of x-ray powder diffraction patterns, which is ascribed to the smaller ionic radius of Te. As for the magnetic properties, firstly the spin state transition of Co^{3+} ions is observed in all samples, and the transition temperature shifts up to higher temperature with Te doping, which is ascribed to the smaller ionic radius and the strong acidity of Te. Secondly, it is interesting that there exists paramagnetic to ferromagnetic phase transition in the Te-doped samples. It is suggested that such a phase transition results from the introduction of Co^{2+} ions and the appearance of double exchange interaction between Co^{2+} and Co^{3+} due to Te doping. Moreover, Curie temperature T_C increases with the increase of the Te doping level x (for $x \leqslant 0.10$), and then decreases with the further increase of x. About the transport properties, the temperature dependence of the resistivity ρ shows that all samples display semiconducting behavior in the whole measured temperature region. And it can be seen that the resistivity first decreases with increasing Te doping level from $x=0$ to 0.10, then increases as $x \geqslant 0.15$. Such variations of T_C and ρ with x are suggested to be related to the structure transition. © *2008 American Institute of Physics*.
[DOI: 10.1063/1.2827494]

INTRODUCTION

Cobalt oxides with perovskite structure have been extensively studied during the second half of the 20th century as a rich family of compounds.[1–4] In these materials, since the Hund's coupling constant J_H and the crystal-field splitting energy 10Dq of Co^{3+} ions are comparable with each other, various spin states such as low-spin (LS) state ($t_{2g}^6 e_g^0$, $S=0$), intermediate-spin (IS) state ($t_{2g}^5 e_g^1$, $S=1$), and high-spin (HS) state ($t_{2g}^4 e_g^2$, $S=2$) are all possible depending on the subtle balance between material parameters J_H and 10Dq as well as the crystal structure and temperature. One representative example is the compound $LaCoO_3$, which exhibits two spin state transitions as the temperature increases. The first transition is from low temperature LS to IS state near 100 K characterized by a steep jump of magnetization at the transition,[5–9] and the second one is from IS to HS state leading to an insulator-metal (I-M) transition around 500 K.[5,10]

The hole-doped cobalt oxides, that divalent ion such as Sr is doped in parent compound $LaCoO_3$, have been studied extensively.[11–13] These obtained results indicate that an I-M transition, accompanied by a change in magnetic properties, occurs for a certain doping concentration. It is usually believed that replacing La^{3+} by Sr^{2+} formally creates Co^{4+} ions and that the double exchange (DE) between Co^{4+} and the remaining Co^{3+} leads to a ferromagnetic (FM) coupling. Yamaguchi *et al.* claimed that Sr doping stabilizes the IS state, resulting in a rapid fade out of the magnetization jump around 100 K.[5] As we know, depending on the type of doping, cobalt ions take three different valence states Co^{2+}, Co^{3+}, and Co^{4+}. In a divalent ion-doped cobalt system, the cobalt ions exist in trivalent and tetravalent states. However, if trivalent rare-earth ions are partially replaced by some tetravalent ions such as tellurium (Te), the corresponding amount of Co^{3+} ions will be converted into Co^{2+} ones and formed electron-doped cobalt oxides. Thereby, one question arises whether there exists DE FM interaction between Co^{3+} and Co^{2+} ions during the substitution of tetravalent ions for trivalent rare-earth ions.

Therefore, we investigate the structural, magnetic, and transport properties of the electron-doped cobalt oxides $La_{1-x}Te_xCoO_3$ in which the trivalent ions La are replaced by the tetravalent ions Te in this paper. A structural transition from rhombohedral ($R\bar{3}C$) to orthorhombic ($Pbnm$) symmetry with Te doping level $x > 0.10$ is found from the x-ray diffraction (XRD) data. The paramagnetic (PM)-FM transition resulting from DE interaction between Co^{2+}–O–Co^{3+} and the spin state transition of Co^{3+} ions are both observed. In addition, the difference between the hole-doped and electron-doped cobaltites is also discussed.

EXPERIMENT

A series of ceramic samples of $La_{1-x}Te_xCoO_3$ ($0 \leqslant x \leqslant 0.25$) were synthesized by a conventional solid-state reaction method in air. The powders mixed in stoichiometric compositions of high-purity La_2O_3, TeO_2, and Co_2O_3 were ground and fired in air at 700 °C for 24 h. The obtained

[a]Electronic mail: ghzheng@issp.ac.cn.

TABLE I. Room temperature structural parameters and the fitting parameters for $La_{1-x}Te_xCoO_3$ ($0 \leqslant x \leqslant 0.25$) samples.

Parameter	$x=0$	$x=0.05$	$x=0.10$	$x=0.15$	$x=0.20$	$x=0.25$
a (Å)	5.5123(1)	5.5030(3)	5.4757(4)	5.3114(5)	5.4219(7)	5.4516(3)
b (Å)	5.5123(1)	5.5030(3)	5.4757(4)	5.3401(1)	5.3389(4)	5.3189(7)
c (Å)	13.2279(2)	13.2450(4)	13.2546(2)	7.5327(7)	7.5448(1)	7.5498(6)
V (Å)^3	348.09(2)	347.36(3)	344.17(2)	213.65(2)	218.40(3)	218.92(6)
Co–O1 (Å)	⋯	⋯	⋯	1.935(2)	1.940(2)	1.942(3)
Co–O2 (Å)	⋯	⋯	⋯	2.036(3)	2.061(2)	2.064(2)
Co–O2 (Å)	⋯	⋯	⋯	1.773(1)	1.788(3)	1.788(4)
⟨Co–O⟩ (Å)	1.969(1)	1.967(2)	1.961(4)	1.914(7)	1.929(7)	1.931(3)
Co–O1–Co (°)	⋯	⋯	⋯	153.37(2)	152.89(2)	152.76(2)
Co–O2–Co (°)	⋯	⋯	⋯	162.60(4)	162.68(4)	162.68(3)
⟨Co–O–Co⟩ (°)	159.03(2)	159.05(2)	159.17(6)	158.52(3)	158.41(7)	158.37(6)
Z	2	2	2	4	4	4
System	Rhombohera ($R\bar{3}C$)	Rhombohera ($R\bar{3}C$)	Rhombohera ($R\bar{3}C$)	Orthorhombic ($Pbnm$)	Orthorhombic ($Pbnm$)	Orthorhombic ($Pbnm$)
R_P (%)	8.23	6.21	7.23	5.56	6.65	8.65

powders were ground, pelletized, and sintered at 1050 °C for 24 h with three intermediate grindings, and finally, the furnace was cooled down to the room temperature. The structure and lattice constant were determined by powder XRD using Cu $K\alpha$ radiation at the room temperature. The resistance using the standard four-probe method was measured in a commercial physical property measurement system (PPMS, $1.9\ \mathrm{K} \leqslant T \leqslant 400\ \mathrm{K}$, $0\ \mathrm{T} \leqslant H \leqslant 9\ \mathrm{T}$) from 100 to 390 K. The magnetic measurements were carried out with a Quantum Design superconducting quantum interference device (SQUID) MPMS system ($1.9\ \mathrm{K} \leqslant T \leqslant 400\ \mathrm{K}$, $0\ \mathrm{T} \leqslant H \leqslant 5\ \mathrm{T}$).

RESULTS AND DISCUSSION

The XRD spectrum at the room temperature shows that all samples are single phase with no detectable secondary phases. XRD patterns of these samples with $x=0$, 0.05, and 0.10 can be indexed by a rhombohedral lattice with the space group $R\bar{3}C$; however, XRD patterns of these samples with $x=0.15$, 0.20, and 0.25 can be indexed by an orthorhombic lattice with the space group $Pbnm$. The structural parameters are refined by the standard Rietveld technique[13] and the fitting between the experimental spectra and the calculated values is every well based on the consideration of low R_p values, as shown in Table I. In Figs. 1(a) and 1(b), the experimental and calculated XRD patterns for these samples with $x=0.10$ and 0.15 are presented, respectively. The fitted structural parameters are listed in Table I. As we can see, for these samples, $La_{1-x}Te_xCoO_3$ ($0 \leqslant x \leqslant 0.25$), the crystal structure at the room temperature changes from a rhombohedral phase ($R\bar{3}C$, $Z=2$, $x \leqslant 0.10$) to an orthorhombic phase ($Pbnm$, $Z=4$, $x > 0.10$).

As we know, Te ion ($r=0.97$ Å) has smaller ionic radius compared with La ion ($r=1.126$ Å). Te doping at La site imposes chemical pressure on the Co ions located at the octahedral center of CoO_6, then makes the bend of the Co–O–Co bond increase, and eventually distorts the crystal structure of the compound. Therefore, it is believed that the crystal structure transition is attributed to the smaller ion Te. Such a crystal symmetry transition from rhomboheral to orthorhombic has also been observed in perovskite cobalt oxides $LaCoO_3$, in which La site is partly substituted by divalent or trivalent ions such as $La_{1-x}Ca_xCoO_3$,[14] $La_{1-x}Sm_xCoO_3$,[15] and $La_{1-x}Eu_xCoO_3$.[16] It is also in accordance with the viewpoint that the orthorhombic structure with $Pbnm$ symmetry is more stable for $ACoO_3$ with a small ionic radius A.[14–16]

Figures 2(a) and 2(b) show the temperature dependence of magnetization $M(T)$ of $La_{1-x}Te_xCoO_3$ ($0 \leqslant x \leqslant 0.25$) at $H=0.05$ T under zero field cooling (ZFC). For $x=0$ sample,

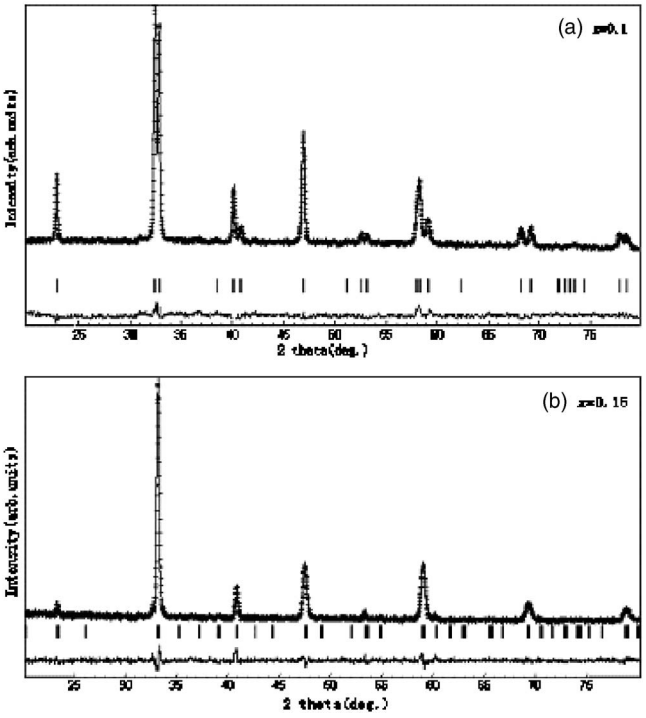

FIG. 1. XRD patterns of $La_{1-x}Te_xCoO_3$ compounds: (a) $x=0.10$ and (b) $x=0.15$. Crosses indicate the experimental data and the calculated data is the continuous line overlapping them. The lowest curve shows the difference between experimental and calculated patterns. The vertical bars indicate the expected reflection positions.

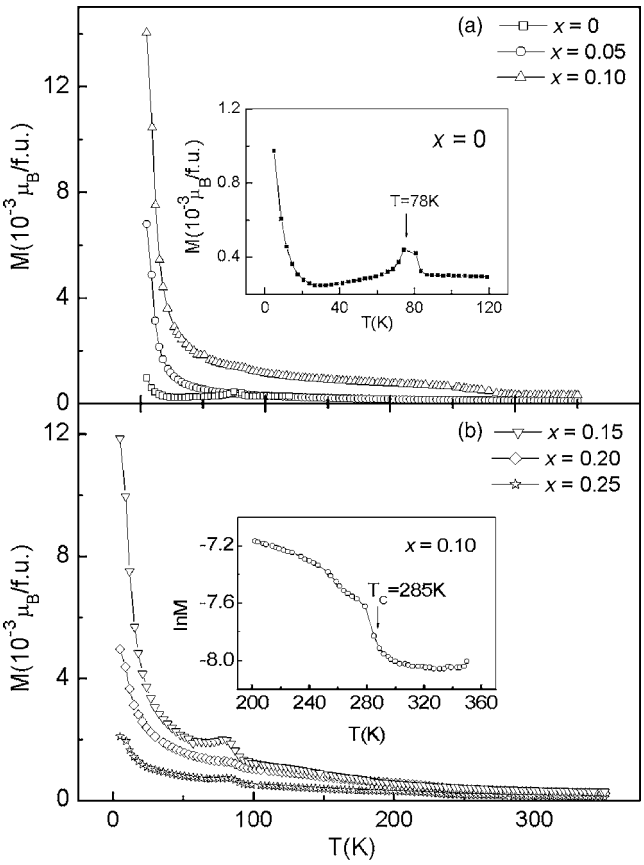

FIG. 2. [(a) and (b)] The temperature dependence of magnetization for $La_{1-x}Te_xCoO_3$ ($0 \leqslant x \leqslant 0.25$) measured at $H=0.05$ T under zero field cooling. The inset of (a) shows M vs T for $x=0$ in the temperature region from 5 to 120 K. The inset of (b) shows ln M vs T for $x=0.10$ in the temperature region from 200 to 360 K.

the $M(T)$ curve exhibits a peak at $T=78$ K in the low temperature region, which corresponds to the spin state transition of Co^{3+} ion from LS to IS.[17] Such a peak can be seen more clearly from the magnified $M(T)$ curve in a small temperature region, as shown in the inset of Fig. 2(a). With Te doping, besides the peak in the low temperature region, M is also observed to increase with the decrease of temperature in the high temperature region, as shown in the M-T curves of Figs. 2(a) and 2(b). The increase of M is related to the PM-FM transition at Curie temperature T_C resulting from Co^{2+}–O–Co^{3+} DE interaction. The PM-FM transition as well as spin state transition will be discussed below in detail.

At first, from $M(T)$ curves for all samples shown in Fig. 2, it can be observed that M increases very rapidly as the temperature decreases in the region below T_{ST}. For Te-free sample $LaCoO_3$, Senarís-Rodríguez *et al.* suggested that the existence of impurity phase Co_3O_4, which contains HS Co^{2+} in tetrahedral sites, leads to the increment of the M in the low temperature region.[10] Corrsepondingly, for the present probed Te-containing compounds, we elucidate that the increase of M with decreasing temperature in the region below T_{ST} is ascribed to the existence of HS Co^{2+} ions due to Te doping.

It is generally believed that Co^{2+} ion always lies in HS state and that such a state does not vary with the doping element, doping level, and temperature as discussed about these compounds, $GdBaCo_2O_5$ and $Ca_3Co_4O_9$.[18–20] Moreover, the peak of the $M(T)$ curve of cobaltites in the range of 25–120 K is always believed to originate from LS to IS transition of Co^{3+} ions. As discussed above, Co^{2+} ions are introduced by Te doping in the $La_{1-x}Te_xCoO_3$ system. That is to say, there exist Co^{2+} and Co^{3+} ions in $La_{1-x}Te_xCoO_3$ samples. Therefore, we conclude that, for these probed samples, the peak in the $M(T)$ curves in the low temperature region is ascribed to the spin state transition of Co^{3+} ions. As mentioned above, a few percentage of Sr doping in $LaCoO_3$ significantly stabilize the HS state of Co^{3+}, resulting in a rapid disappearance of magnetization peak at ~110 K.[5] In other words, a doped hole causes locally the low-to-high-spin state transition of Co ions, which is interpreted that hole doping in the low-spin ground state of $LaCoO_3$ leads to the formation of localized polarons with unusually high-spin number.[5] Therefore, it is reasonable to deduce that a doped electron is made against the formation of such localized polarons with unusually high-spin number, and that it eventually stabilizes the LS state of Co^{3+} ions in the electron-doped samples. This is why we observe the spin state transition in the electron-doped cobaltites $La_{1-x}Te_xCoO_3$. the corresponding transition temperature is defined as T_{ST}. With increasing x, T_{ST} gradually increases from 78 K for $x=0$ to 84 K for $x=0.25$, as presented in Table II. Obviously, the presence of Te^{4+} ions shifts T_{ST} up to higher temperature. There exist two possible ingredients related to the increase of T_{ST}. Firstly, the partial substitution of La^{3+} by the smaller ionic radius Te^{4+} systematically increases the chemical pressure, which enhances the crystal-field splitting and eventually stabilizes the LS state of Co^{3+} ions. Therefore, the higher thermal activation energy is needed to overcome the larger energy gap of spin state transition. As a result, T_{ST} moves up to higher temperature with increasing Te doping level. It is also evidenced that the spin state transition in $RCoO_3$ systems with small radius ions such as Lu^{3+} occurs at higher temperature above 500 K.[21] Secondly, Te atom has strong acidity. The strong acidity makes Te atom compete strongly with cobalt to bond with the oxygen atoms. Such a competition

TABLE II. Magnetic and transport parameters of $La_{1-x}Te_xCoO_3$ ($0 \leqslant x \leqslant 0.25$) samples.

Parameter	$x=0$	$x=0.05$	$x=0.10$	$x=0.15$	$x=0.20$	$x=0.25$
T_{ST} (K)	78	80	81	82	83	84
T_C (K)	⋯	275	285	250	233	230
$(T_0)_1$	9.67×10^7	2.07×10^8	1.28×10^8	5.63×10^8	1.88×10^9	⋯
$(T_0)_2$	4.34×10^8	⋯	⋯	⋯	⋯	⋯

results in a progressive stabilization of the π^* (Co–O) levels and a large splitting between t_{2g} and e_g levels, and thus Co ions are in LS states.[10]

For the PM-FM transition observed in the Te-containing samples, we speculate above that it may result from the Co^{2+}–O–Co^{3+} DE interaction. For the sake of clarity, we plot the temperature T dependence of M in logarithmic scale for the $x=0.10$ sample in the temperature region from 200 to 360 K, as shown in the inset of Fig. 2(b). The Curie temperatures T_C are 275, 285, 250, 233, and 230 K for $x=0.05$, 0.10, 0.15, 0.20, and 0.25, respectively, which are listed in Table II. T_C firstly increases with increasing Te doping level for $x \leqslant 0.10$ and decreases with increasing Te doping level further. Then there exists a T_C maximum at $x=0.10$, correspondingly. The increase of T_C and the strengthening of the FM interactions can be analyzed from the Rietveld refinement results. From Table I, we can clearly find that the Co–O–Co angle is about 159.05° and 159.17°, and that the Co–O bond lengths are 1.967 and 1.961 Å for $x=0.05$ and 0.10 samples, respectively. These structural parameters suggest that the Co–O bond length decreases and that the Co–O–Co bond angle increases slightly with increasing Te doping level as $x \leqslant 0.10$. With increasing x further from 0.15 to 0.25, the A-site average ionic radius $\langle r_A \rangle$ decreases. In such a doping range, the Co–O–Co bond angle derivates significantly from 180°, yielding a reduced effective d-d electron transfer via the O_{2p} states, and thus resulting in the reduction of T_C. At $x=0.10$, corresponding to the appearance of maximum T_C, there also occurs a structural transition, as discussed above. Therefore, it is reasonable to deduce that the variation of T_C with x is related to the structural transition. Compared with the previously reported hole-doped cobaltites, the PM-FM transition and the FM interaction are weak in the current electron-doped samples. The largest difference between the two kinds of doped systems is the combination of valence of Co ions, i.e., Co^{3+}/Co^{4+} for hole-doped one and Co^{2+}/Co^{3+} for electron-doped one. Yamaguchi *et al.* claimed that the FM-metallic state in the hole-doped cobaltites is composed by mobile high-spin polarons.[5] As presented above, Te doping stabilizes the LS state of Co^{3+} ions in the electron-doped samples. Therefore, there are a few mobile high-spin polarons to compose FM state, as a result, weak FM interaction and PM-FM transition are observed in the current $La_{1-x}Te_xCoO_3$ samples.

Although Co^{2+} ion is always believed to be in HS state, Co^{3+} ion has three different spin states and the spin state configuration changes with temperature, doping element, and concentration as reported in $R_{0.67}Sr_{0.33}CoO_3$.[22] Therefore, it is necessary to determine the variation of Co^{3+} ion spin state with doping level and temperature. As well known, for a ferromagnet in the PM region, the relation between χ_m and the temperature T should follow the Curie-Weiss law, i.e., $\chi_m = C/(T-\Theta)$, where χ_m is the magnetic susceptibility, C is the Curie constant, and Θ is the Curie-Weiss temperature. For all Te-containing samples, the experimental data in PM region can be fitted well according to the Curie-Weiss law. Taking the sample with $x=0.20$ as an example, $1/\chi_m$ vs T is presented in the inset of Fig. 3. Based on the slope value of the fitting curve $1/\chi_m$ vs T, the average Co spin value S_{avg} is obtained. The S_{avg} as a function of Te doping level x is plotted in Fig. 3.

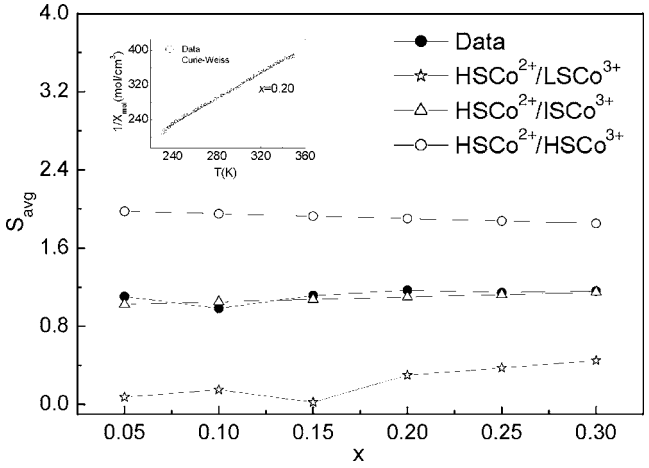

FIG. 3. x dependence of the average Co spin value (S_{avg}) extracted from the Curie-Weiss behavior in the PM region. The inset shows χ^{-1} vs $T(T>T_C)$ for $x=0.20$. Solid line is the fitting result according to Curie-Weiss law.

If the spins of Co^{2+} and Co^{3+} ion are denoted as S^{2+} and S^{3+}, respectively. For $La_{1-x}Te_xCoO_3$, S_{avg} can be described as $S_{avg}=(1-x)S^{3+}+xS^{2+}=S^{3+}+x(S^{2+}-S^{3+})$. Considering that Co^{2+} ion is always believed to lie in the HS state and that Co^{3+} ion has three different spin states, we plot S_{avg} values corresponding to three different spin state configurations of Co^{3+} in Fig. 3. From this figure, one can find that S_{avg} values corresponding to the assumption that $HSCo^{2+}/ISCo^{3+}$ matches the experimental data well. Moreover, we observe that S_{avg} values change slightly with x, and that there is almost no variation in the spin state within the doping range of $0.05 \leqslant x \leqslant 0.25$. Therefore, it is reasonable to conclude that Co^{2+} is in the HS state and Co^{3+} is in the IS state in the PM region for all Te-containing samples, which is consistent with the electron-doped cobaltites $La_{1-x}Ce_xCoO_3$.[27]

To gain more insight into the magnetic behavior, we measured the field H dependence of M at 5 K from 0 to 4.5 T for all samples. The results are shown in Figure 4. For all samples, M increases drastically below 1 T but does not reach saturation up to 4.5 T, possibly indicating the existence of the antiferromagnetic (AFM) component. From Figure 4, one finds that $M(H)$ dependence deviates linear behavior for all these samples, which implies there exists a weak FM interaction in samples. Previous reports show that there are AFM exchange interactions between the Co ions with the same valence, and that FM exchange interactions between the Co ions with different valences.[23,24] In the current samples, there exist HS Co^{2+} and LS Co^{3+} ions below $T_{ST}(T=5\ \text{K} < T_{ST})$. Therefore, AFM interaction is possibly introduced between Co^{3+} and Co^{3+}, and Co^{2+} and Co^{2+}, and the weak FM comes from the DE interaction between Co^{2+}–O–Co^{3+}. However, there are many other reasons, such as itinerant ferromagnetism and grain boundaries, resulting in reduced magnetization, and the proper determination of the magnetic properties of the materials should be performed by neutron diffraction experiment in the further investigations. From Fig. 4, it is also seen that the magnitude of mag-

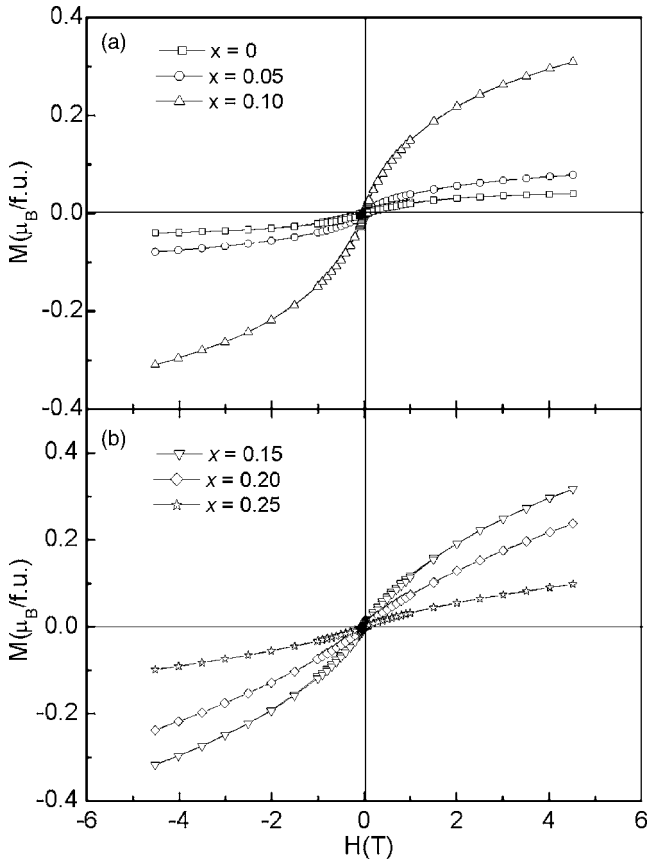

FIG. 4. Field dependence of the magnetization $M(H)$ for the compound $La_{1-x}Te_xCoO_3$ ($0 \leqslant x \leqslant 0.25$) at 5 K.

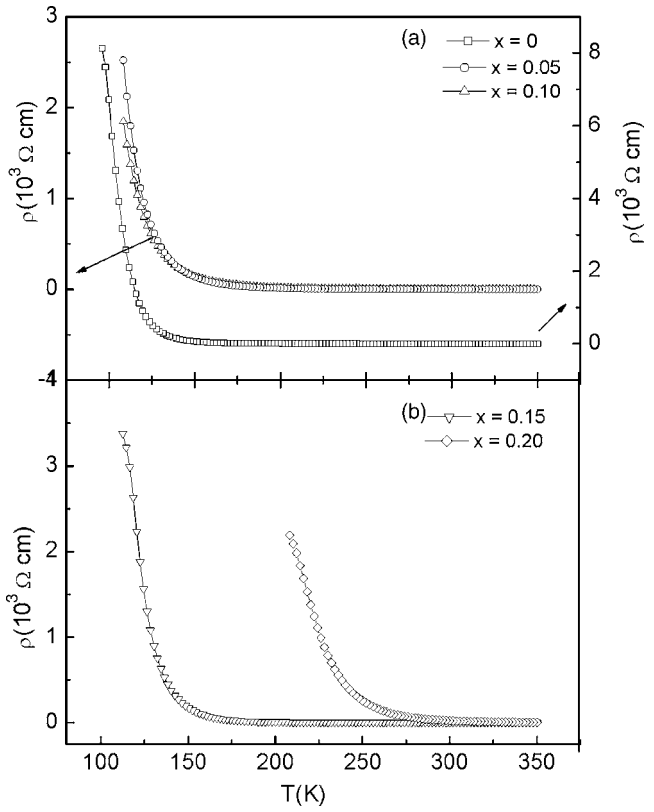

FIG. 5. The temperature dependence of the resistivity $\rho(T)$ of $La_{1-x}Te_xCoO_3$ ($0 \leqslant x \leqslant 0.25$) samples at zero field.

netization M at any field at 5 K exhibits the same variation tendency with the deviation of the slop $M(H)$. And the deviation of the slop increases firstly with increasing Te doping level, reaches a maximum value at $x=0.10$, then decreases with the further increase of doping level.

As we all know, in cobalt oxides, the comparable J_H and 10Dq lead to the coexistence of HS, IS, and LS states of Co ions and the transition between these spin states. And this kind of spin state transition has a complex influence on the properties of the cobalt oxides. Based on the $M(T)$ and $M(H)$ curves, shown in Figs. 2 and 4, we have suggested that the FM ordering is of short range in cobalt oxides, which implies the weak FM interaction between Co ions. Such a conclusion can also be evidenced from the resistivity discussed below.

To investigate the effect of Te doping on the transport properties of $LaCoO_3$ compounds, the temperature dependence of resistivity ρ is measured for the samples with $x=0$, 0.05, 0.10, 0.15, and 0.20 at zero field in the temperature range of 100–350 K. The result is shown in Fig. 5. In contrast to the I-M transition accompanied with the PM-FM phase transition observed in the hole-doped cobaltites,[11–13] from this figure it can be seen that $\rho(T)$ curves of all measured samples display semiconducting behaviors. It is in accordance with the above discussion that both PM-FM transition and FM interaction in the electron-doped cobaltites are weaker than those in the hole-doped ones. The weak FM interaction is not in favor of the mobility of e_g electrons, and, hence, the resistivity follows semiconducting behaviors in both FM and PM phases in $La_{1-x}Te_xCoO_3$ samples. It is also seen that the resistivity decreases with x, reaches a minimum at $x=0.10$, then increases with increasing Te doping level further. The resistivity becomes too high below 100 K to be measured by PPMS. For the sample with $x=0.25$, it cannot be measured at any temperature because of its too high resistance value. The decrease of resistivity with increasing x for $x \leqslant 0.10$ is ascribed to the introduction of DE interaction, which is in favor of the mobility of e_g electrons. As Te doping level increases from 0.15 to 0.25, the resistivity increases. This can be discussed as follows. Firstly, with increasing Te doping level further, the deviation of Co–O–Co bond angle from 180° increases, and FM DE interaction weakens, then the hopping probability of charge carriers decreases, and eventually the resistivity increases corrspondingly. Secondly, it has been mentioned[25,26] that the IS state of Co^{3+} can be stabilized by the hybridization between the Co $3d$ and the O $2p$ states. Te doping stabilizes the LS state of Co^{3+} relative to the IS state; as a result, the decrease of Co$3d$ and O$2p$ hybridization with increasing Te doping level is also reflected by the increase of resistivity. In order to test whether the $La_{1-x}Te_xCoO_3$ samples have magnetoresistance (MR), the resistivity is also measured at an applied field of 5 T for the samples with $x=0$, 0.05, 0.10, 0.15, and 0.20 in the temperature range of 100–350 K (not shown here). The obtained results indicate that no MR is observed in these samples. No anomalous signatures corresponding to T_{ST} and T_C in $\rho(T)$ curves are observed for all samples. Generally, FM and metallic conduction must coexist within the framework of the DE model. However, as mentioned above, the

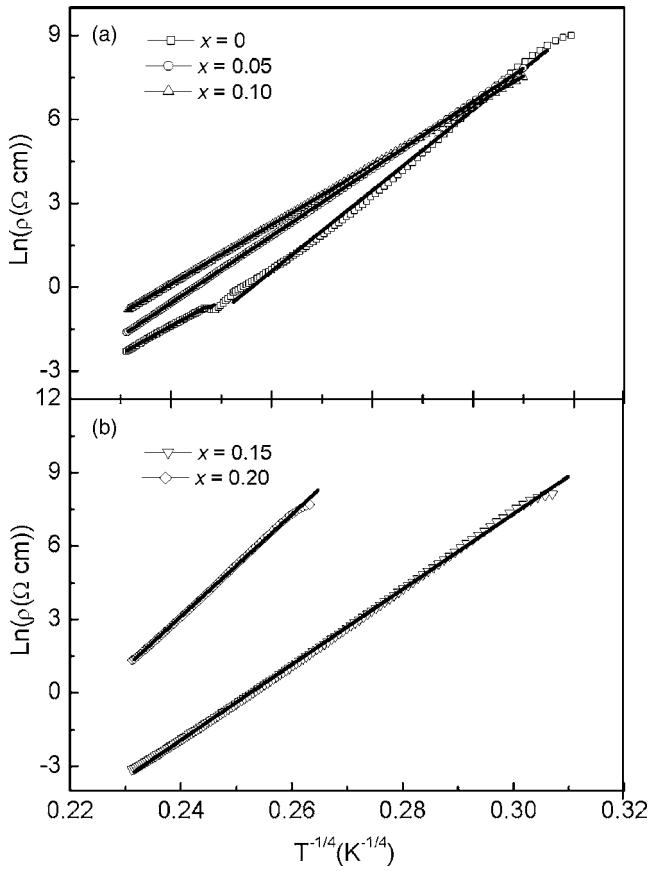

FIG. 6. The fitting and experimental resistivity curves at the zero field for $La_{1-x}Te_xCoO_3$ ($0 \leqslant x \leqslant 0.25$) according to the VRH model. The lines represent the fitting data.

FM ordering is characterized as short range in these $La_{1-x}Te_xCoO_3$ samples. FM metal phases are disconnected because of the existence of insulating phases among them, which results in no I-M transition in $\rho(T)$ curves observed for all measured samples.

In order to understand better the electronic transport mechanism for all measured samples, the resistivity data in the whole measured temperature region are fitted by (i) the thermally activated (TA) law $[\rho \sim \exp(E_0/k_BT)]$, (ii) the adiabatic small polaron hopping (SPH) model $[\rho \sim T\exp(E_P/k_BT)]$, and (iii) the variable range hopping (VRH) model $[\rho \sim \exp(T_0/T)^{1/4}]$.[27] The fitting results show that $\rho(T)$ curves of the samples with $x \geqslant 0.05$ can be well described by VRH model, as presented in Fig. 6. However, for Te-free sample, it is well fitted by two different fitting parameters of $(T_0)_1$ and $(T_0)_2$ in the different temperature ranges. In Table II, we show the fitting parameter T_0, which is a characteristic temperature related to the localization length ξ and the density of the states $N(E_F)$ in the vicinity of the Fermi energy level, i.e., $k_BT_0 \approx 21/[\xi^3 N(E_F)]$. From this table, it is found that T_0 decreases initially with increasing Te doping content from 0.05 to 0.10 and then increases for $x \geqslant 0.15$, and that there exists a minimum value at 0.10. The decrease of T_0 with increasing Te doping level from 0.05 to 0.10 implies the increase of the localization length, which results in the decrease of the resistivity. With increasing the doping level further, the T_0 value increases obviously, implying the decrease of the localization length and the reduction of the carrier mobility, and it is intimately related to the increase of resistivity as $x \geqslant 0.15$, which is in accordance with the magnetic and electronic transport properties for the study samples.

CONCLUSION

In summary, we have investigated the effect of Te doping at La site on structural, magnetic, and transport properties of perovskite cobalt oxides $La_{1-x}Te_xCoO_3$ ($0 \leqslant x \leqslant 0.25$) by measuring XRD patterns, magnetization, and resistance. The room temperature structural transition from rhombohedra ($R\bar{3}C$) to orthorhombic ($Pbnm$) symmetry is found in the samples with $x \geqslant 0.15$ by the Rietveld refinement of XRD patterns. The Co^{3+} ion spin state transition from LS to IS is observed for all samples and the transition shifts to higher temperatures with Te doping. The PM to FM transition is observed for Te-containing samples, and T_C increases firstly with increasing Te doping level for $x \leqslant 0.10$ and then decreases. The measured magnetization values for these Te-containing samples suggest Co^{2+} ion lies in HS state and Co^{3+} ion lies in IS state in the PM state. The resistivity $\rho(T)$ for all samples displays semiconducting behaviors in the whole measured temperature range. Moreover, Te doping makes the resisitvity decrease as $x \leqslant 0.10$, which originates from the Co^{2+}–O–Co^{3+} DE interaction due to Te doping. With increasing Te doping level further, the resisitvity increases which is explained as the combined effects of the deviation of Co–O–Co bond and the decrease of Co3d and O2p hybridization.

ACKNOWLEDGMENTS

This work was supported by the National Key Research under Contract No. 001CB610604, the National Nature Science Foundation of China under Contract Nos. 10474100 and 10374033, the Fundamental Bureau of the Chinese Academy of Sciences, and Anhui College provincial level natural sciences research Project No. KJ2007B130.

[1] W. C. Koehler and E. O. Wollan, J. Phys. Chem. Solids **2**, 100 (1957).
[2] J. B. Goodenough, J. Phys. Chem. Solids **6**, 287 (1958).
[3] M. Zhuang, W. Y. Zhang, and N. B. Ming, Phys. Rev. B **57**, 10705 (1998).
[4] S. Yamaguchi, Y. Okimoto, and Y. Tokura, Phys. Rev. B **55**, R8666 (1997).
[5] S. Yamaguchi, Y. Okimoto, H. Taniguchi, and Y. Tokura, Phys. Rev. B **53**, R2926 (1996).
[6] P. Raccah and J. Goodenough, Phys. Rev. **155**, 932 (1967).
[7] V. Bhide, D. Rajoria, G. R. Rao, V. Jadhao, and C. Rao, Phys. Rev. B **6**, 1021 (1972).
[8] Y. Kobayashi, N. Fujiwara, S. Murata, K. Asai, and H. Yasuoka, Phys. Rev. B **62**, 410 (2000).
[9] T. Saitoh, T. Mizokawa, A. Fujimori, M. Abbate, Y. Takeda, and M. Takano, Phys. Rev. B **55**, 4257 (1997).
[10] M. Senarís-Rodríguez and J. Goodenough, J. Solid State Chem. **116**, 224 (1995).
[11] A. Chainani, M. Mathew, and D. Sarma, Phys. Rev. B **46**, 9976 (1992).
[12] R. Mahendiran and A. K. Raychaudhuri, Phys. Rev. B **54**, 16044 (1996).
[13] D. B. Wiles and R. A. Young, J. Appl. Crystallogr. **14**, 149 (1981).
[14] J. C. Burley, J. F. Mitchell, and S. Short, Phys. Rev. B **69**, 054414 (2004).
[15] J. R. Sun, R. W. Li, and B. G. Shen, J. Appl. Phys. **89**, 1331 (2001).
[16] J. Caier, S. Jodlauk, M. Kriener, A. Reichl, C. Zobel, H. Kierspel, A. Freinmuth, and T. Lorenz, Phys. Rev. B **71**, 014443 (2005).
[17] P. R. Heikes, R. C. Miller, and R. Mazelsky, Physica (Amsterdam) **30**,

1600 (1964); V. G. Bhide, S. Rajoria, G. R. Rao, and C. N. Rao, Phys. Rev. B **6**, 1021 (1972).
[18]A. Maignan, V. Caigaert, B. Raveau, D. Khomskii, and G. Sawatzky, Phys. Rev. Lett. **93**, 026401 (2004).
[19]D. D. Khalyavin, S. N. Barilo, S. V. Shiryaev, G. L. Bychkov, and I. O. Troyanchuk, Phys. Rev. B **67**, 214421 (2003).
[20]J. Sugiyama, C. T. Xia, and T. Tani, Phys. Rev. B **67**, 104410 (2003).
[21]M. Demazeau, M. Pouchard, and P. Hagenmuller, J. Solid State Chem. **9**, 202 (1974).
[22]M. Paraskevopoulos, J. Hemberger, A. Krimmel, and A. Loidl, Phys. Rev. B **63**, 224416 (2001).
[23]M. A. Senaris-Rodriguez and J. B. Goodernogh, J. Solid State Chem. **118**, 323 (1995).
[24]G. H. Jonker and J. H. Vsnten, Physica (Amsterdam) **19**, 120 (1953).
[25]M. A. Korotin, S. Yu. Ezhov, I. V. Solovyev, and V. I. Anisimov, Phys. Rev. B **54**, 5309 (1996).
[26]I. A. Nekrasov, S. V. Streltsov, M. A. Korotin, and V. I. Anisimov, Phys. Rev. B **68**, 235113 (2003).
[27]A. Sundaresan, A. Maignan, and B. Raveau, Phys. Rev. B **56**, 5092 (1997).